The Astrophysical Journal, 657: L25–L28, 2007 March 1

VLA AND *XMM-NEWTON* OBSERVATIONS OF THE SNR W41/TeV GAMMA-RAY SOURCE HESS J1834−087

W. W. Tian,[1,2] Z. Li,[3] D. A. Leahy,[2] and Q. D. Wang[3]

Received 2006 December 11; accepted 2007 January 9; published 2007 January 22

ABSTRACT

The recently discovered extended TeV source HESS J1834−087 is associated with both a diffuse X-ray enhancement and a molecular cloud, projected at the center of an old radio supernova remnant, G23.3−0.3 (SNR W41). New H I observations from the VLA Galactic Plane Survey (VGPS) show unambiguous structures associated with W41 in the radial velocity range of 53–63 km s^{-1}, so we obtain for W41 a distance of 4 ± 0.2 kpc. A new higher sensitivity VGPS continuum image of W41 at 1420 MHz shows faint emission in its eastern part not detected by previous observations, so we provide a new angular size of 36′ × 30′ in the *b*-*l* direction (average radius of 19 pc). We estimate for W41 an age of ~10^5 yr. A new *XMM-Newton* observation reveals diffuse X-ray emission within the HESS source and suggests an association between the X-ray and γ-ray emission. The high-resolution ^{13}CO images of W41 further reveal a giant molecular cloud (GMC) located at the center of W41, likely associated with W41 in the radial velocity range of 61–66 km s^{-1}. Altogether, the new observations can be interpreted as providing the first evidence that an old SNR encounters a GMC to emit TeV γ-rays in the cloud material.

Subject headings: gamma rays: observations — ISM: molecules — radio continuum: galaxies — radio lines: galaxies — supernova remnants — X-rays: galaxies

Online material: color figures

1. INTRODUCTION

Young supernova remnants (SNRs) are one of the main galactic populations to generate very high energy (above 10^{11} eV) γ-rays (Torres et al. 2003). Observationally, TeV γ-rays have been detected from the Crab Nebula (SN 1054; Weekes et al. 1989) and the SNRs RX J1713.7−3946 (G347.3−0.5; Enomoto et al. 2002) and RX J0852.0−4622 (G266.2−1.2; Aharonian et al. 2005a). Theoretically, acceleration mechanisms for relativistic electrons at SNR shock fronts have been well established (Malkov & Drury 2001). Recently, the survey of Aharonian et al. (2006) of the inner part of our Galaxy has revealed 14 new TeV γ-ray sources. The origin of some of them remains uncertain. Yamazaki et al. (2006) showed that TeV γ-rays can originate from an old SNR of an age around 10^5 yr or from a giant molecular cloud (GMC) encountered by the SNR, via pion decay from proton-proton collisions. In their scenario, the flux ratio of the γ-rays to the associated X-ray emission is much higher than that from a young SNR. In this Letter, we provide observational evidence supporting the theory that an old SNR encounters a GMC to emit TeV γ-rays, based on new radio and X-ray observations as well as recent ^{13}CO images of SNR W41, which is spatially coincident with HESS J1834−087, one of the 14 TeV sources.

2. RADIO AND X-RAY OBSERVATIONS

The radio continuum and H I emission data sets come from the Very Large Array (VLA) Galactic Plane Survey (VGPS), described in detail by Stil et al. (2006). The data sets are mainly based on observations from VLA of the National Radio Astronomy Observatory (NRAO). The spatial resolution of the continuum images of W41 is 1′ (FWHM) at 1420 MHz. The synthesized beam for the H I line images is 1′, and the radial velocity resolution is 1.56 km s^{-1}. The short-spacing information for the H I spectral line images is from additional observations with the 100 m Green Bank Telescope of the NRAO.

W41 was observed by *XMM-Newton* on 2005 September 18 (ObsID 0302560301; principal investigator: G. Puehlhofer), with a 20 ks exposure. In this work, we only used data obtained from the EPIC-pn. We used SAS, version 7.0.0, for data reduction. We selected pn events with patterns 0–4 and applied flag filter FLAG = 0. Excluding time intervals contaminated by background flares results in a net exposure of 12.4 ks. We then constructed exposure maps in the 0.3–0.7, 0.7–1.5, 1.5–3, and 3–7 keV bands for flat-fielding. We applied the "filter wheel closed" data for instrumental background subtraction. We also searched for pointlike sources using a detection procedure detailed by Wang (2004).

3. RESULTS

3.1. *Continuum Emission*

The VGPS continuum image of W41 at 1420 MHz is shown in Figure 1. The VGPS map has a higher resolution (by a factor of 3) and sensitivity and shows more details than the previous image at 330 MHz (Kassim 1992). A prominent filament structure outlines W41. Fainter features, not detected by previous observations, appear in its eastern part. The new image gives a corrected angular size of W41: 36′ × 30′ in the *b*-*l* direction. The H II regions overlapping in W41 have been resolved into at least three components. We have derived an integrated flux density of 59.7 ± 8.2 Jy for W41 (including H II regions in the SNR) at 1420 MHz. The resulting 330–1420 MHz spectral index (the flux density is 143 ± 29 Jy at 330 MHz including H II regions; Kassim 1992) has a lower limit of 0.43 ($S_\nu \propto \nu^{-\alpha}$). The TeV γ-ray source HESS J1934−087, detected by Aharonian et al. (2005b), is located at the center of W41. Its location and extent are shown by a white circle, centered at (l, b) = (23.24°, −0.32°) with a radius of 5.4′ (Aharonian et al. 2006). The pulsar PSR J1933−0827, also shown in Figure 1, was proposed to be associated with W41 by Gaensler & Johnston (1995).

[1] National Astronomical Observatories, Chinese Academy of Sciences, Beijing, China.
[2] Department of Physics and Astronomy, University of Calgary, Calgary, AB, Canada; tww@iras.ucalgary.ca.
[3] Department of Astronomy, University of Massachusetts, Amherst, MA.

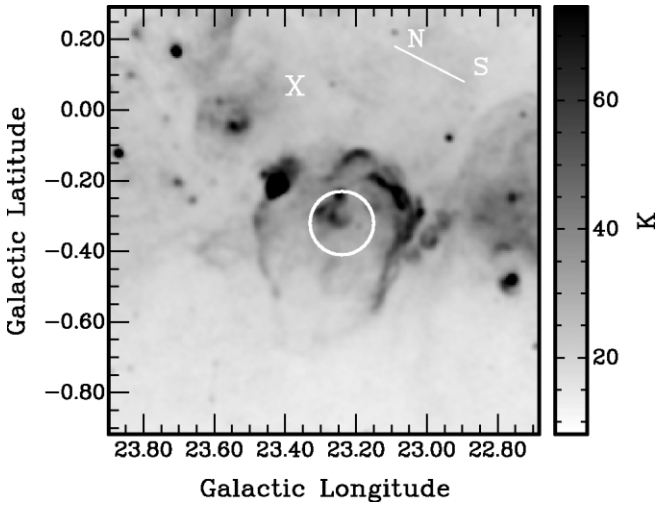

FIG. 1.—VGPS continuum image of W41 at 1420 MHz. The central circle shows the position and extent of the TeV γ-ray HESS J1934−087. The pulsar PSR J1933−0827 is marked by a cross. The directions of north (N) and south (S) are marked.

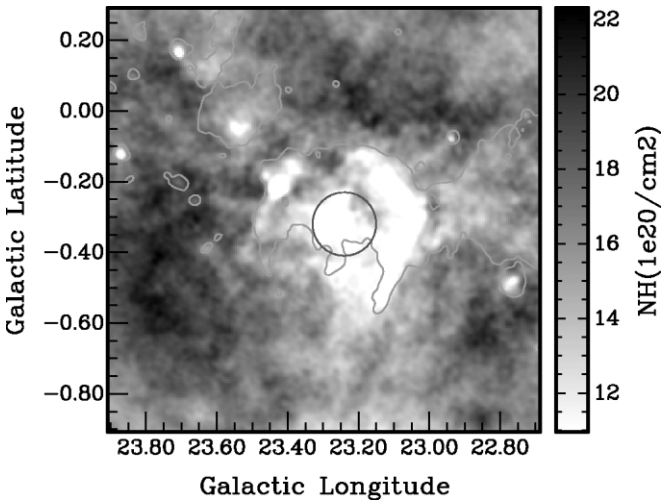

FIG. 2.—Column density map of the VGPS H I line emissions associated with W41. This map has superimposed W41's contour at 30 K of continuum emission at 1420 MHz chosen to show the SNR (*contours*). The circle shows the position and extent of HESS J1834−087. [*See the electronic edition of the Journal for a color version of this figure*.]

3.2. H I *and* CO *Emission*

We have searched the VGPS radial velocity range for features in the H I that might be related to the morphology of W41. There is unambiguous H I emission coincident with the SNR in the velocity range 53–63 km s^{-1}. Figure 2 is the column density map of H I emission integrated over channels from 53 to 63 km s^{-1} in units of 10^{20} atoms cm^{-2}. The map has superimposed the 30 K contour of 1420 MHz continuum emission chosen to show the SNR. The circle is the same as in Figure 1.

We extract ^{13}CO images of W41 from the survey of Jackson et al. (2006). A GMC is found at the center of W41 and in the radial velocity range of 61–66 km s^{-1}, so it is highly likely associated with W41. Figure 3 shows the averaged ^{13}CO map for channels from 61 to 66 km s^{-1}. The contour and circle in the map are the same as in Figure 2.

3.3. *X-Ray Emission*

The X-ray images of W41 are shown in Figure 4 for the soft (0.3–1.5 keV) and hard (3–7 keV) bands. In the soft band, the bulk of the field is of smooth, low intensity. In the hard band, a region of enhanced intensities is clearly present within the extent of HESS J1834−087. With the resolution of the instrument (FWHM $\sim 13''$), the enhancement is apparently extended by visual comparison with nearby point sources in the range, although we cannot completely rule out the possibility that it represents an unusual cluster of pointlike sources. Given its location, this feature is likely associated with HESS J1834−087.

We perform spectral analysis for the feature, for which we extract a spectrum from a circle centered at (l, b) = (23.243°, −0.331°) with a radius of 2.5′ (Fig. 4). To determine the local sky background, we extract a spectrum from a concentric circle with a radius of 7.5′ and with the enclosed circle representing HESS J1834−087 and detected pointlike sources excluded. The two spectra are shown in Figure 5. Part of the background emission may arise from the interior of the remnant and vary between the source and background regions. Thus, our procedure of background determination might be affected by this nonuniformity. Nevertheless, encouraged by the apparently uniform surface intensity at energies below 1.5 keV (Fig. 4), we assume that the background emission also varies little at higher energies. We use the X-ray spectral fitting package XSPEC to fit the background spectrum and find that it can be characterized by a combined model consisting of a thermal plasma component (APEC in XSPEC) and a power-law component, both subject to absorption (Table 1). These two components, scaled accordingly to the sky area, are applied to account for the background contribution in the source spectrum. The remaining emission in the source spectrum, presumably intrinsic to the feature, is then characterized by an additional component, for which we find a heavily absorbed power law. Fitting results are listed in Table 1.

4. DISCUSSION AND CONCLUSION

4.1. *Distance and Age of W41*

Using flat galactic rotation velocity $V_R = V_0 = 200$ km s^{-1} and $R_0 = 8.0$ kpc, we obtain the SNR's distance of 4 ± 0.2 kpc or 10.7 ± 0.2 kpc. The updated average angular diameter of W41, 33′, yields a radius of about $R = 19$ pc ($d = 4$ kpc) or 51 pc ($d = 10.7$ kpc) for the SNR. Since known shell-type SNRs are

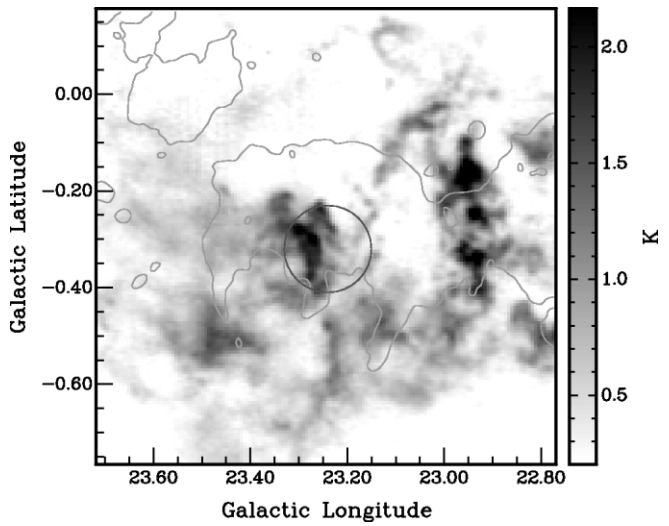

FIG. 3.—Averaged ^{13}CO emission in the field centered on W41 from 61 to 66 km s^{-1}. The contours and circle in the map have the same meaning as in Fig. 2. [*See the electronic edition of the Journal for a color version of this figure*.]

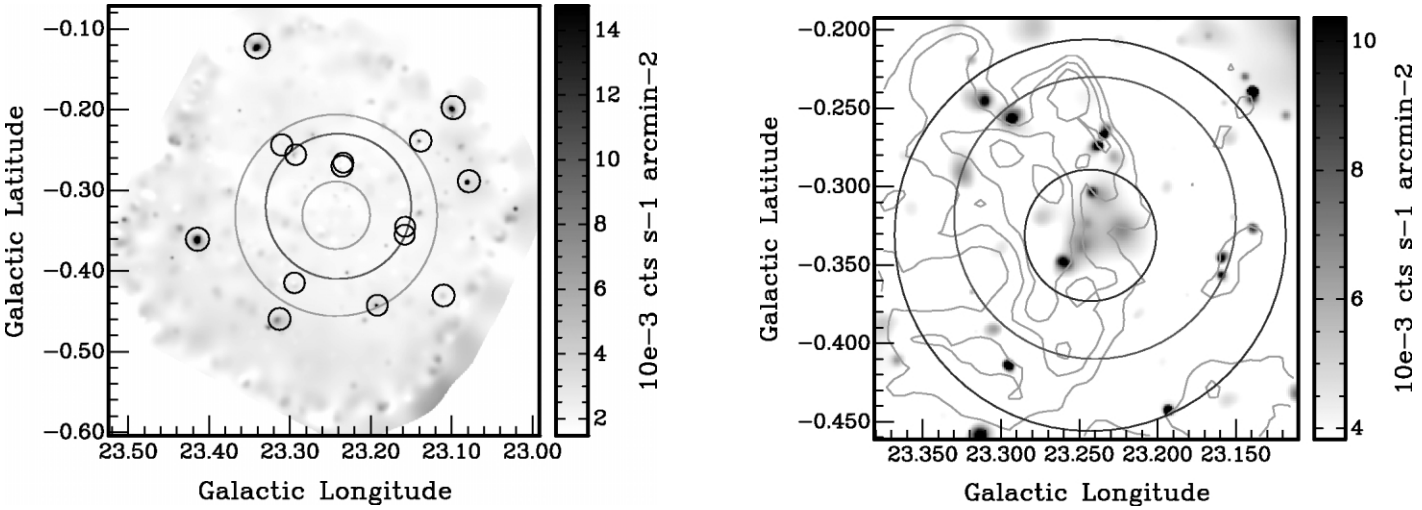

FIG. 4.—*XMM-Newton* EPIC-pn intensity images of SNR W41 in the 0.3–1.5 keV (*left*) and 1.5–7 keV (*right*) bands. The intensity is adaptively smoothed using *csmooth* to achieve a signal-to-noise ratio of ~3. The middle circle represents the location and extent of the γ-ray source HESS J1834−087. The small circle illustrates the region of spectral interest, while the large circle outlines the region (with the enclosed middle circle excluded) where the background spectrum is extracted. The smaller circles (*left*) outline detected sources and their extent according to twice the 50% encircled energy radius, which are excluded from spectral extraction. The right plot has superimposed contours of ^{13}CO emission from Fig. 3, at 0.8, 1.2, 1.6 and 2.1 k. [*See the electronic edition of the Journal for a color version of this figure*.]

a few to ~20 pc in radius, we adopt the closer distance. From the H I column density map associated with W41 (Fig. 2), we estimate a $N_{\rm H}$ of about (5–10) × 10^{20} cm^{-2}, so the density $n_0 = N_{\rm H}/2R$ around W41 is about 6 cm^{-3}. Applying a Sedov model (Cox 1972), for a typical explosion energy of $E = 0.75 \times 10^{51}$ ergs, yields an age of ~6 × 10^4 yr. However, for $n_0 \sim 6$ cm^{-3}, one finds $R > R_s^{(c)}$ (the radius for complete cooling; Cox 1972). The age determined from the complete cooling expansion is ~2 × 10^5 yr.

4.2. *X-Ray, TeV Gamma-Ray, and* CO *Emission from W41*

Previous ^{12}CO observations have shown that W41 is associated with a very large molecular complex (Dame et al. 1986). Albert et al. (2006) studied the ^{12}CO images from Dame et al. (2001) and suggested that the GMC associated with W41 is best defined by the integrated ^{12}CO peak emission from 70 to 85 km s^{-1}. They also used the ^{13}CO images from Jackson et al. (2006) and confirmed that the recently discovered TeV source HESS J1834−087 lies toward a GMC. However, our observations show the H I line emissions are associated with W41 in the velocity range of 53–63 km s^{-1}. ^{13}CO is useful as an optically thin tracer of the molecular cloud, so we reanalyzed the ^{13}CO images of W41. We found a GMC located at the center of W41 in the radial velocity range of 61–66 km s^{-1}. Figure 3 shows the bright ^{13}CO emission in the velocity range and that it is coincident with HESS J1834−087. The total H_2 mass of the CO emission peak (over a 0.1° × 0.2° region) is estimated from $M_{\rm H_2} = N_{\rm H_2}\Omega d^2(2m_{\rm H}/M_\odot)$. We take $N_{\rm H_2}/W_{\rm CO} \approx 1.8 \times 10^{20}$ cm^{-2} K^{-1} km^{-1} s from Dame et al. (2001). The total integrated intensity of ^{13}CO is $W_{\rm CO} \approx 5$ K km s^{-1} from Figure 3. Assuming a ^{12}CO/^{13}CO isotopic abundance ratio of 30 (Langer & Penzias 1990), we obtain an average H_2 column density of $N_{\rm H_2} \approx 2.7 \times 10^{22}$ cm^{-2} and a molecular cloud mass of $M_{\rm H_2} \approx 4.5 \times 10^4\ M_\odot$. This is a GMC with a density of ~10^3 cm^{-3}.

From the observed γ-ray luminosity (Albert et al. 2006), using equation (16) in Torres et al. (2003) and a supernova power of 10^{51} ergs, we obtain a relation between an acceleration efficiency θ of hadrons and the required density n of matter in the γ-ray production region for a hadronic origin of the observed radiation: $\theta \sim 10^{-2}$ requires $n \sim 10^2$ cm^{-3}; $\theta \sim 10^{-3}$ requires $n \sim 10^3$ cm^{-3} (similar values are obtained by Combi et

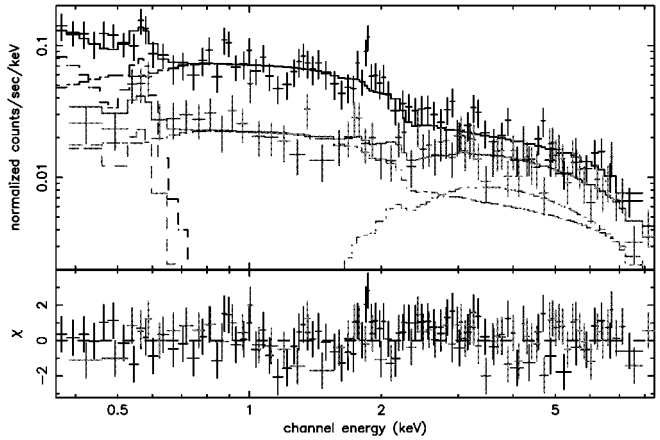

FIG. 5.—EPIC-pn spectra from the SNR W41 region. *Gray*: Spectrum of the X-ray feature associated with HESS J1834−087. *Black*: Spectrum of local sky background. The spectra are instrumental background-subtracted and are binned to achieve a signal-to-noise ratio better than 3. Also shown are the best-fit models (*solid curves*) to the spectra and the different model components (*dashed and dotted curves*). See text for details. [*See the electronic edition of the Journal for a color version of this figure*.]

TABLE 1
FIT TO THE X-RAY SPECTRUM

Parameter	Value
χ^2/degrees of freedom	61.3/74
$N_{\rm H,1}$ (10^{20} cm^{-2})	3.0 (<9.0)[a]
Temperature (keV; APEC)	$0.09^{+0.03}_{-0.02}$
Photon index (PL1)	$0.80^{+0.13}_{-0.11}$
$N_{\rm H,2}$ (10^{22} cm^{-2})	$6.2^{+3.1}_{-2.5}$
Photon index (PL2)	$2.0^{+0.7}_{-0.8}$
Flux (10^{-13} ergs s^{-1} cm^{-2})[b]	7.0

NOTE.—A combined model of absorbed ($N_{\rm H,1}$) APEC+power law (PL1) is used for characterizing the sky background, and a second absorbed ($N_{\rm H,1}$) power law (PL2) is used to model to the emission from the feature.

[a] Quoted uncertainties are at the 90% confidence level.

[b] A 2–10 keV intrinsic flux for PL2.

al. [1998] for another SNR likely interacting with a massive cloud). Generally, the maximum acceleration efficiency θ of 10% is accepted, so the GMC is dense enough to produce the observed TeV intensity with a lower acceleration efficiency. The protons could diffuse only partway into the cloud, resulting in the observed offset of peak CO and p-p to π^0 decay TeV γ-rays. The physical peak of X-ray and TeV should be coincident. The column density of the molecular cloud is enough to absorb X-rays and cause the offset to the right of the observed X-ray peak with respect to the likely true peak of the emission.

HESS J1834−087 has an extended nature, as revealed by the Major Atmospheric Gamma Imaging Cerenkov (MAGIC) telescope and High Energy Stereoscopic System (HESS) observations (Albert et al. 2006; Aharonian et al. 2006). From the *Swift* X-Ray Telescope observations of W41, Landi et al. (2006) found a faint X-ray source within the extent of HESS J1834−087 and thereby suggested a possible pulsar wind nebula (PWN) association. This X-ray source, located at (l, b) = (23.2340°, −0.2657°), is also detected by the present *XMM-Newton* observation, but there is no evidence for the existence of a PWN. Instead, the prominent diffuse X-ray feature is most likely associated with the TeV γ-ray emission.

Yamazaki et al. (2006) studied the X-ray and γ-ray emission from evolved SNRs with an age of around 10^5 yr and that from a GMC interacting with the SNR. They showed that TeV γ-ray emission can originate from the SNR, or from the SNR shock running into a GMC, or from the GMC illuminated by high-energy protons from the SNR shock. These different origins may be distinguished by the X-ray to γ-ray spectra. A simple diagnostic is the ratio of the γ-ray to the X-ray flux, $R_{\rm TeV/X} = F_\gamma(1\text{–}10\ {\rm TeV})/F_{\rm X}(2\text{–}10\ {\rm keV})$. According to Yamazaki et al. (2006), for the three cases (in the above-mentioned order), the value of $R_{\rm TeV/X}$ is of order 10–10^2, 10, and >10^2, respectively, for their fiducial SNR parameters. For young SNRs found to show γ-ray emission, $R_{\rm TeV/X}$ is typically below ∼2. For HESS J1834−087, the 1–10 TeV γ-ray flux is ∼8 × 10^{-12} ergs s^{-1} cm^{-2}, based on the MAGIC observation (Albert et al. 2006). Our 2–10 keV X-ray flux is ∼7 × 10^{-13} ergs s^{-1} cm^{-2}, giving $R_{\rm TeV/X} \simeq 11$, with uncertainty of a factor of 2. HESS J1834−087 is possibly arising from a shocked GMC. This is supported by the presence of the GMC as found from the ^{13}CO detection. The velocities indicate that the GMC is just behind W41. The absorption column density of a few times 10^{22} cm^{-2} estimated from the X-ray spectral fit (Table 1) also implies that the nonthermal X-ray emission associated with HESS J1834−087 arises from within the GMC and is behind W41. According to Yamazaki et al. (2006), the X-ray emission from a shocked GMC or a GMC illuminated by high-energy protons is likely synchrotron emission from secondary electrons arising from hadronic processes. The hard X-ray spectrum that we find is also consistent with such a scenario.

Pulsar J1833−0827 (b = 23.386°, l = 0.063°) lies at the north side and about 10′ away from the edge of W41. It has a kinematic distance of 4–5 kpc by H I absorption (Weisberg et al. 1995) and a dispersion measure distance of 5.7 kpc and a characteristic age of 147 kyr (Taylor et al. 1993).

Our results for the distance (4 kpc) and age (∼10^5 yr) of W41 are consistent with the pulsar J1833−0827 and support the possible associations W41/PSR J1833−0827 also. However, the pulsar is about 20′ away from the extended γ-ray source and is not associated with HESS J1834−087.

W. W. T. and D. A. L. acknowledge support from the Natural Sciences and Engineering Research Council of Canada. The research at the University of Massachusetts is supported by the NASA *Chandra* X-Ray Center under grant GO5-6057X. W. W. T. appreciates support from the Natural Science Foundation of China. We thank R. Kothes for helpful discussions and J. M. Stil for providing the VGPS data. This publication makes use of molecular line data from the Boston University–FCRAO Galactic Ring Survey. The NRAO is a facility of the National Science Foundation operated under cooperative agreement by Associated Universities, Inc.

REFERENCES

Aharonian, F., et al. 2005a, A&A, 437, L7
———. 2005b, Science, 307, 1938
———. 2006, ApJ, 636, 777
Albert, J., et al. 2006, ApJ, 643, L53
Combi, J. A., Romero, G. E., & Benaglia, P. 1998, A&A, 333, L91
Cox, D. 1972, ApJ, 178, 159
Dame, T. M., Elmegreen, B. G., Cohen, R. S., & Thaddeus, P. 1986, ApJ, 305, 892
Dame, T. M., Hartmann, D., & Thaddeus, P. 2001, ApJ, 547, 792
Enomoto, R., Tanimori, T., & Naito, T. 2002, Nature, 416, 823
Gaensler, B. M., & Johnston, S. 1995, MNRAS, 275, L73
Jackson, J. M., et al. 2006, ApJS, 163, 145
Kassim, N. E. 1992, AJ, 103, 943
Landi, R., Bassani, L., & Malizia, A. 2006, ApJ, 651, 190
Langer, W. D., & Penzias, A. A. 1990, ApJ, 357, 477
Malkov, E., & Drury, L. O'C. 2001, Rep. Prog. Phys., 64, 429
Stil, J. M., et al. 2006, AJ, 132, 1158
Taylor, J. H., Manchester, R. N., & Lyne, A. G. 1993, ApJS, 88, 529
Torres, D. F., Romero, G. E., Dame, T. M., Combi, J. A., & Butt, Y. M. 2003, Phys. Rep., 382, 303
Wang, Q. D. 2004, ApJ, 612, 159
Weekes, T. C., et al. 1989, ApJ, 342, 379
Weisberg, J. M., Siegel, M. H., Frail, D. A., & Johnston, S. 1995, ApJ, 447, 204
Yamazaki, R., Kohri, K., Bamba, A., Yoshida, T., Tsuribe, T., & Takahara, F. 2006, MNRAS, 371, 1975